Ion firehose instability in plasmas with plasma particles described by product bi-kappa distributions

M. S. dos Santos, L. F. Ziebell, and R. Gaelzer

Citation: Physics of Plasmas (1994-present) **21**, 112102 (2014); doi: 10.1063/1.4900766
View online: http://dx.doi.org/10.1063/1.4900766
View Table of Contents: http://scitation.aip.org/content/aip/journal/pop/21/11?ver=pdfcov
Published by the AIP Publishing

Ion firehose instability in plasmas with plasma particles described by product bi-kappa distributions

M. S. dos Santos, L. F. Ziebell,[a] and R. Gaelzer[b]
Instituto de Física, Universidade Federal do Rio Grande do Sul, Caixa Postal 15051, RS, CEP: 91501-970 Porto Alegre, Brasil

(Received 5 August 2014; accepted 20 October 2014; published online 3 November 2014)

We investigate the dispersion relation for low frequency electromagnetic waves propagating parallel to the ambient magnetic field, considering that the velocity distributions of ions and electrons can be either bi-Maxwellian of product bi-kappa distributions. The effect of the anisotropy and non-thermal features associated to the product-bi-kappa distributions on the firehose instability are numerically investigated. The general conclusion to be drawn from the results obtained is that the increase in non-thermal features which is consequence of the decrease of the κ indexes in the ion distribution contributes to increase the instability in magnitude and wave number range, in comparison with bi-Maxwellian distributions with similar temperature anisotropy, and that the increase of non-thermal features in the electron distribution contributes to the quenching of the instability, which is nevertheless driven by the anisotropy in the ion distribution. Significant differences between results obtained either considering product-bi-kappa distributions or bi-kappa distributions are also reported. [http://dx.doi.org/10.1063/1.4900766]

I. INTRODUCTION

The ion firehose instability is an instability associated with velocity dispersion along parallel velocity which is larger than the velocity dispersion along perpendicular direction. For plasma particles with bi-Maxwellian velocity distributions, for which the temperature is a measure of the velocity dispersion, it can be said that the ion firehose instability is associated with the condition $T_{i\perp}/T_{i\|} < 1$, where i indicates the ion population.[1,2] The ion firehose instability has been traditionally described by considering anisotropic Maxwellian distributions, as in a previous investigation by some of us, which has taken into account the presence of dust.[3] The subject has been object of continued interest, particularly from the community interested in physical processes in space plasmas. Discussion on the conditions for the occurrence of the instability, particularly on the constraints related to the temperature anisotropies, can be easily found in recent literature.[4,5]

On the other hand, many observations show that plasma particles in space conditions frequently display non-thermal tails and anisotropies which are not well described by Maxwellian distributions.[6–9] It has been realized that these non-thermal features can be better described by the use of distributions with power-law tails, generally known as *kappa distributions*.[10–14] These kappa distributions can be isotropic, and in that case are usually written in two different forms, with basic features which can be found, respectively, in Refs. 10–12 and 13, 14. The abundance of evidence of non-thermal features in velocity distributions of plasma particles in spatial environments has lead to a growing interest in the study of spatial phenomena considering the presence of kappa distributions.[15] For instance, it can be mentioned that several studies about low-frequency electromagnetic instabilities have been recently made considering the presence of kappa distributions, either dealing with the ion-cyclotron instability[16,17] or with the ion firehose instability.[18–20] The occurrence of instabilities like these requires the presence of anisotropic features, which have to be incorporated to the description of the velocity distribution functions. For the mentioned studies regarding instabilities, the anisotropy which drives the instability has been generally described by the adoption of particle distributions with anisotropic parameters related to the temperature, with a single kappa index, which constitute the use of distributions which are known as Bi-Kappa (BK) Distributions.[16–20] However, the use of BK distributions is not the only form of introduction of anisotropic features in power-law velocity distributions. A more general description of anisotropic and non-thermal features can be made with the use of distributions which, in addition to anisotropic temperature parameters, are described by anisotropic kappa indexes. These distributions are known as Product-Bi-Kappa (PBK) distributions. Product-bi-kappa distributions have been already mentioned in analysis of the space plasma dynamics and on the limits for the occurrence of instabilities associated to different forms of the distributions,[21] but they are not yet widely found in studies of the plasma instabilities, particularly in studies dedicated to the ion firehose instability. However, as we have argued, PBK distributions are very flexible with respect to the possibility of description of anisotropic non thermal features in velocity distributions, and feature desirable mathematical properties, like the separability of perpendicular and parallel variables. Therefore, they can be of utility for fitting observed features in particle velocity distributions, such as electron distributions with *strahl* or double-*strahl* components, or double-humped ion distributions.[6,7,9] These characteristics are particularly

[a]Electronic mail: luiz.ziebell@ufrgs.br
[b]Electronic mail: rudi.gaelzer@ufrgs.br

difficult to model using bi-Maxwellian or even bi-kappa distributions. The mentioned attractive features of PBK distributions therefore motivate the present investigation.

In the present paper, we study the dispersion relation for the ion firehose instability, considering that the velocity distributions of ions and electrons can be either bi-Maxwellian or product bi-kappa distributions. We obtain the general form of the dispersion relation and then discuss the numerical solution considering different situations. The organization of the paper is as follows: In Sec. II, we briefly describe the theoretical formulation and the dispersion relation for electromagnetic waves propagating parallel to the ambient magnetic field, considering the particular cases of plasma particles with product-bi-kappa and bi-Maxwellian distribution functions. In Sec. III, we present and discuss results obtained by numerical solution of the dispersion relation. Final remarks and a discussion on future perspectives appear in Sec. IV.

II. THEORETICAL FORMULATION

The general dispersion relation for parallel propagation follows from the following determinant:

$$\det\begin{pmatrix} 1+\chi_{xx}-N_\parallel^2 & \chi_{xy} & 0 \\ -\chi_{yx} & 1+\chi_{xx}-N_\parallel^2 & 0 \\ 0 & 0 & 1+e_{zz} \end{pmatrix} = 0\,, \quad (1)$$

where

$$\chi_{xx} = \frac{1}{4}\sum_\beta \frac{\omega_{p\beta}^2}{\omega^2}\frac{1}{n_{\beta 0}}\sum_{n=-1,1} J(n,1,0;f_{\beta 0}),$$

$$\chi_{xy} = i\,\frac{1}{4}\sum_\beta \frac{\omega_{p\beta}^2}{\omega^2}\frac{1}{n_{\beta 0}}\sum_{n=-1,1} nJ(n,1,0;f_{\beta 0}) = i\,\xi_{xy},$$

$$e_{zz} = -\sum_\beta \frac{\omega_{p\beta}^2}{\omega^2}\frac{1}{n_{\beta 0}}\int d^3u\,\frac{v_\parallel}{v_\perp}\mathcal{L}(f_{\beta 0}) + \sum_\beta \frac{\omega_{p\beta}^2}{\omega^2}\frac{1}{n_{\beta 0}}J(0,0,2;f_{\beta 0}),$$

and where

$$J(n,m,h;f_{\beta 0}) \equiv \omega\int d^3v\,\frac{v_\parallel^h v_\perp^{2(m-1)} v_\perp L(f_{\beta 0})}{\omega - n\Omega_\beta - k_\parallel v_\parallel}\,,$$

$$L = \left[\left(1-\frac{k_\parallel v_\parallel}{\omega}\right)\frac{\partial}{\partial v_\perp} + \frac{k_\parallel v_\perp}{\omega}\frac{\partial}{\partial v_\parallel}\right], \quad (2)$$

$$\mathcal{L} = v_\parallel\frac{\partial}{\partial v_\perp} - v_\perp\frac{\partial}{\partial v_\parallel}\,,$$

with

$$\omega_{p\beta}^2 = \frac{4\pi n_{\beta 0}q_\beta^2}{m_\beta}\,, \quad \Omega_\beta = \frac{q_\beta B_0}{m_\beta c}\,, \quad N_\parallel = \frac{ck_\parallel}{\omega}.$$

The dispersion relation for Alfvén waves is obtained retaining only the components in the upper left 2×2 determinant in Eq. (1), that is, by imposing $E_z = 0$,

$$(1+\chi_{xx}-N_\parallel^2)^2 - \xi_{xy}^2 = 0.$$

By squaring this expression, two possibilities of sign ($s=\pm 1$) are obtained, and it is easy to show that the dispersion relation becomes s-dependent, as follows:

$$N_\parallel^2 = 1 + \frac{1}{2}\sum_\beta \frac{\omega_{p\beta}^2}{\omega^2}\frac{1}{n_{\beta 0}}J(s,1,0;f_{\beta 0}). \quad (3)$$

For the application to be developed in the present paper, we consider the case of anisotropic kappa distributions for electrons and ions, characterized by anisotropic kappa indexes,

$$f_{\beta,\kappa}(v_\parallel,v_\perp) = \frac{n_{\beta 0}}{\pi^{3/2}\kappa_{\beta\perp}\kappa_{\beta\parallel}^{1/2}v_{\beta\perp}^2 v_{\beta\parallel}} \times \frac{\Gamma(\kappa_{\beta\perp})\Gamma(\kappa_{\beta\parallel})}{\Gamma(\kappa_{\beta\perp}-1)\Gamma(\kappa_{\beta\parallel}-1/2)} \times \left(1+\frac{v_\parallel^2}{\kappa_{\beta\parallel}v_{\beta\parallel}^2}\right)^{-\kappa_{\beta\parallel}}\left(1+\frac{v_\perp^2}{\kappa_{\beta\perp}v_{\beta\perp}^2}\right)^{-\kappa_{\beta\perp}}, \quad (4)$$

where

$$v_{\beta\parallel}^2 = \frac{2T_{\beta\parallel}}{m_\beta}, \quad v_{\beta\perp}^2 = \frac{2T_{\beta\perp}}{m_\beta}.$$

In order to avoid negative arguments in the Γ functions, the range of values of the κ indexes has to be restricted to $\kappa_\parallel > 0.5$ and $\kappa_\perp > 1.0$. Anisotropic distributions like that of Eq. (4) are also called "product bi-kappa" distributions, to be distinguished from the distributions characterized by a single kappa index and anisotropic temperature parameters T_β, which are called "bi-kappa" or "bi-Lorentzian" distributions.[11,18]

We define the effective temperature using energy units, such that the average value of the kinetic energy per unit of volume, along each degree of liberty, is $nT_{\rm eff}/2$. The effective temperatures along parallel and perpendicular directions will be denoted as $\theta_\parallel$ and $\theta_\perp$, respectively.

Therefore, the effective temperatures along parallel and perpendicular directions, for particles of species β, will be obtained from

$$\begin{pmatrix}\frac{1}{2}\theta_{\beta\parallel}\\ \theta_{\beta\perp}\end{pmatrix} = \frac{m_\beta}{\pi^{1/2}\kappa_{\beta\perp}\kappa_{\beta\parallel}^{1/2}v_{\beta\perp}^2 v_{\beta\parallel}}\frac{\Gamma(\kappa_{\beta\perp})\Gamma(\kappa_{\beta\parallel})}{\Gamma(\kappa_{\beta\perp}-1)\Gamma(\kappa_{\beta\parallel}-1/2)} \times \int_{-\infty}^{\infty} dv_\parallel\left(1+\frac{v_\parallel^2}{\kappa_{\beta\parallel}v_{\beta\parallel}^2}\right)^{-\kappa_{\beta\parallel}} \times \int_0^\infty dv_\perp v_\perp\left(1+\frac{v_\perp^2}{\kappa_{\beta\perp}v_{\beta\perp}^2}\right)^{-\kappa_{\beta\perp}}\begin{pmatrix}v_\parallel^2\\ v_\perp^2\end{pmatrix}. \quad (5)$$

Upon evaluation of the integral, the outcome is as follows:

$$\theta_{\beta\parallel} = \frac{\kappa_{\beta\parallel}}{(\kappa_{\beta\parallel}-3/2)}T_{\beta\parallel}, \quad (6)$$

$$\theta_{\beta\perp} = \frac{\kappa_{\beta\perp}}{(\kappa_{\beta\perp}-2)}T_{\beta\perp}, \quad (7)$$

and therefore, the ratio of effective temperatures is given by

$$\frac{\theta_{\beta\perp}}{\theta_{\beta\parallel}} = \frac{\kappa_{\beta\perp}\left(\kappa_{\beta\parallel} - 3/2\right)}{\kappa_{\beta\parallel}\left(\kappa_{\beta\perp} - 2\right)} \frac{T_{\beta\perp}}{T_{\beta\parallel}}. \tag{8}$$

In what follows, the quantities $\theta_{\beta\perp}$ and $\theta_{\beta\parallel}$ will be denominated "effective temperatures," and the quantities $T_{\beta\perp}$ and $T_{\beta\parallel}$ will be denominated "temperatures," for simplicity. Of course, in the case of a Maxwellian distribution, when $T_{\beta\perp} = T_{\beta\parallel}$, the quantities $T_{\beta\perp}$ and $T_{\beta\parallel}$ represent the true thermodynamical temperature of the distribution, along the indicated directions.

It is convenient, at this point, to introduce dimensionless variables

$$\begin{aligned} z &= \frac{\omega}{\Omega_*}, \quad q_\parallel = \frac{k_\parallel v_*}{\Omega_*}, \quad q_\perp = \frac{k_\perp v_*}{\Omega_*}, \\ r_\beta &= \frac{\Omega_\beta}{\Omega_*}, \quad u_{\beta\parallel}^2 = \frac{v_{\beta\parallel}^2}{v_*^2}, \quad u_{\beta\perp}^2 = \frac{v_{\beta\perp}^2}{v_*^2}, \end{aligned} \tag{9}$$

where Ω_* and v_* are some characteristic angular frequency and velocity, respectively. For the present application, which is concerned with the dispersive properties of Alfvén waves, we make the convenient choice $v_* = v_A$, the Alfvén velocity, and $\Omega_* = \Omega_i$, the angular ion cyclotron frequency.

Using the distribution function given by Eq. (4), the integral defined in Eq. (2) may be evaluated, leading to the following:[22]

$$\begin{aligned} J(s,1,0;f_{\beta 0}) = 2n_{\beta 0} &\frac{\kappa_{\beta\perp}}{\kappa_{\beta\perp} - 2} \\ &\times \left[-\frac{\kappa_{\beta\perp} - 2}{\kappa_{\beta\perp}} + \frac{u_{\beta\perp}^2}{u_{\beta\parallel}^2} \frac{\kappa_{\beta\parallel} - 1/2}{\kappa_{\beta\parallel}} \right. \\ &+ \left(\zeta_\beta^0 - \zeta_\beta^s\right) \frac{\kappa_{\beta\perp} - 2}{\kappa_{\beta\perp}} Z_{\kappa_{\beta\parallel}}^{(0)}\left(\zeta_\beta^s\right) \\ &\left. + \frac{u_{\beta\perp}^2}{u_{\beta\parallel}^2} \zeta_\beta^s Z_{\kappa_{\beta\parallel}}^{(1)}\left(\zeta_\beta^s\right) \right], \end{aligned} \tag{10}$$

where

$$\zeta_\beta^n = \frac{z - n r_\beta}{q_\parallel u_{\beta\parallel}} \qquad \zeta_\beta^0 = \frac{z}{q_\parallel u_{\beta\parallel}},$$

and where we have introduced the plasma dispersion function of order m, defined for distributions with a κ parameter,

$$\begin{aligned} Z_\kappa^{(m)}(\xi) = &\frac{1}{\pi^{1/2}} \frac{\Gamma(\kappa)}{\kappa^{1/2}\Gamma(\kappa - 1/2)} \\ &\times \int_{-\infty}^{\infty} \frac{ds}{(s - \xi)(1 + s^2/\kappa)^{\kappa + m}}. \end{aligned} \tag{11}$$

This plasma dispersion function can be written in terms of the Gauss hypergeometric function ${}_2F_1(a, b, c; z)$, as follows:

$$\begin{aligned} Z_\kappa^{(m)}(\xi) = &\frac{i\Gamma(\kappa)\Gamma(\kappa + m + 1/2)}{\kappa^{1/2}\Gamma(\kappa - 1/2)\Gamma(\kappa + m + 1)} \\ &\times {}_2F_1\left[1, 2\kappa + 2m, \kappa + m + 1; \frac{1}{2}\left(1 + \frac{i\xi}{\kappa^{1/2}}\right)\right], \end{aligned} \tag{12}$$

for $\kappa > -m - 1/2$. For $m = 1$, the plasma dispersion function given by Eqs. (11) and (12) is the same as the dispersion function defined by Summers and Thorne (1991) and Mace and Hellberg (1995).[11,12]

The value of the integral J for the case of a bi-Maxwellian distribution function can be obtained as a limiting case of Eq. (10), for $\kappa_\perp \to \infty$, $\kappa_\parallel \to \infty$. In this limiting case the plasma dispersion of order m becomes the well-known Z function, $\lim_{\kappa\to\infty} Z_\kappa^{(m)}(\zeta) = Z(\zeta)$, and the J integral becomes

$$\begin{aligned} J(s,1,0;f_{\beta 0}) = 2n_{\beta 0} &\left[-1 + \frac{u_{\beta\perp}^2}{u_{\beta\parallel}^2} \right. \\ &\left. + \left(\zeta_\beta^0 - \zeta_\beta^s\right) Z\left(\zeta_\beta^s\right) + \frac{u_{\beta\perp}^2}{u_{\beta\parallel}^2} \zeta_\beta^s Z\left(\zeta_\beta^s\right) \right]. \end{aligned} \tag{13}$$

When ions and electrons are described by a product-bi-kappa distribution as given by Eq. (4), the dispersion relation (3) can be written as follows:

$$\begin{aligned} N_\parallel^2 = 1 + \frac{1}{z^2} \sum_\beta \frac{\omega_{p\beta}^2}{\Omega_i^2} &\left[-1 + \frac{\kappa_{\beta\perp}}{\kappa_{\beta\perp} - 2} \frac{\kappa_{\beta\parallel} - 1/2}{\kappa_{\beta\parallel}} \frac{u_{\beta\perp}^2}{u_{\beta\parallel}^2} \right. \\ &\left. + \left(\zeta_\beta^0 - \zeta_\beta^s\right) Z_{\kappa_{\beta\parallel}}^{(0)}\left(\zeta_\beta^s\right) + \frac{\kappa_{\beta\perp}}{\kappa_{\beta\perp} - 2} \frac{u_{\beta\perp}^2}{u_{\beta\parallel}^2} \zeta_\beta^s Z_{\kappa_{\beta\parallel}}^{(1)}\left(\zeta_\beta^s\right) \right]. \end{aligned} \tag{14}$$

In the limiting case of $\kappa_{\beta\perp} \to \infty$, $\kappa_{\beta\parallel} \to \infty$, the dispersion relation becomes that corresponding to bi-Maxwellian distributions

$$\begin{aligned} N_\parallel^2 = 1 + \frac{1}{z^2} \sum_\beta \frac{\omega_{p\beta}^2}{\Omega_i^2} &\left[-1 + \frac{u_{\beta\perp}^2}{u_{\beta\parallel}^2} \right. \\ &\left. + \left(\zeta_\beta^0 - \zeta_\beta^s\right) Z\left(\zeta_\beta^s\right) + \frac{u_{\beta\perp}^2}{u_{\beta\parallel}^2} \zeta_\beta^s Z\left(\zeta_\beta^s\right) \right]. \end{aligned} \tag{15}$$

In the case of isotropic temperatures, the dispersion relation is further simplified and becomes the well-known dispersion relation for low-frequency parallel propagating electromagnetic waves in a thermal plasma

$$N_\parallel^2 = 1 + \sum_\beta \frac{\omega_{p\beta}^2}{\omega^2} \zeta_\beta^0 Z\left(\zeta_\beta^s\right). \tag{16}$$

Of course, if one particle species is characterized by a product-bi-kappa distribution and the other species is characterized by an anisotropic Maxwellian, the dispersion relation (14) has to be used with a combination of Eqs. (10) and (13).

III. NUMERICAL ANALYSIS

For the numerical analysis which follows, we have considered $v_A/c = 1.0 \times 10^{-4}$ and $\beta_i = 2.0$, values which have been used in well-known studies on space plasmas instabilities.[1] We have also considered ion mass equal to proton mass, and ion charge number $Z_i = 1.0$. For all cases which are shown, the electron temperature has been taken as equal to the ion parallel

temperature, $T_e = T_{i\|}$. We have also added a figure with some results obtained considering $\beta_i = 1.0$, in order to illustrate the effect of the change of the β parameter.

We have solved the dispersion relation for different forms of the distribution functions for electrons and ions. In the figures, we show the imaginary part of the normalized frequency, for waves in the whistler branch, investigating the effect of anisotropy in the effective temperature of the ions on the ion firehose instability.

In Figure 1, we show the imaginary part of the normalized wave frequency (z_i) vs. normalized wave number, obtained from the solution of the dispersion relation, considering isotropic Maxwellian distribution for electrons and different forms of the ion distribution. The column to the left shows the values of the growth rate γ, the positive values of z_i, while the right column shows the complete range of values of z_i. Figures 1(a) and 1(e) show the results obtained for the case in which the ions are described by an anisotropic Maxwellian distribution, with $T_{i\perp}/T_{i\|} = 0.1$, 0.2, 0.3, 0.4, 0.5, 0.6, 0.7, 0.8, 0.9, and 1.0. It is seen that instability only occurs for temperature ratio less than 0.8. For $T_{i\perp}/T_{i\|} = 0.1$, which is the smaller value of the temperature ratio with results shown in the figure, the instability starts at $q \simeq 0.22$ and continues until beyond $q = 1.8$. For larger values of $T_{i\perp}/T_{i\|}$ the unstable range decreases and the magnitude of the growth rate decreases as well, so that for $T_{i\perp} = 0.5T_{i\|}$ the instability occurs between $q \simeq 0.3$ and $q \simeq 0.7$, with maximum growth rate which is slightly below one tenth of the maximum attained for temperature ratio 0.1. The situation depicted in Figure 1(a) corresponds to the conventional firehose instability.

Figures 1(b) and 1(f) consider the case in which the ions are described by a product-bi-kappa distribution, with $\kappa_{i\|} = \kappa_{i\perp} = 20$, and the same values of $T_{i\perp}/T_{i\|}$ considered in the case of Figure 1(a), with $T_e = T_{i\|}$. The corresponding values of the ratio of effective temperatures for the curves featuring instability are $\theta_{i\perp}/\theta_{i\|} = 0.103$, 0.206, 0.308, 0.411, 0.514, 0.617, and 0.719, values which are close to those of the temperature ratios. The curves representing γ and z_i which are shown in Figures 1(b) and 1(f) are very similar in shape to those appearing in Figures 1(a) and 1(e), with two noticeable differences. It is noticed that the values of γ at the peak of the instability are slightly above those obtained in the Maxwellian case, shown in Figure 1(a), and that the unstable range is slightly larger than in the Maxwellian case, starting at a smaller value of q. The similarity between the results in (a) and (b) is not surprising, since the product bi-kappa-distribution with $\kappa_{i\|} = \kappa_{i\perp} = 20$, considered in the case of panel (b), is not very different from a Maxwellian distribution. Perhaps the most noticeable difference associated to the lingering non-thermal character of the product-bi-kappa distribution in this case of high kappa values is the tendency to extension of the unstable region toward $q = 0$, for sufficiently small value of the ratio $T_{i\perp}/T_{i\|}$.

In Figures 1(c) and 1(g), we depict the results obtained considering the ions described by a product-bi-kappa distribution, with $\kappa_{\|} = \kappa_{\perp} = 5.0$ and $T_e = T_{i\|}$, and $T_{i\perp}/T_{i\|}$ ranging between 0.1 and 1.0, the same values of $T_{i\perp}/T_{i\|}$ used to obtain Figures 1(a) and 1(b). The corresponding ratios of effective temperatures are $\theta_{i\perp}/\theta_{i\|} = 0.117$, 0.233, 0.350, 0.467, 0.583, 0.700, 0.817, 0.933, 1.050, and 1.167. It is interesting to notice that the effective anisotropy is reversed for $T_{i\perp}/T_{i\|} \geq 0.9$, approximately, so that Figure 1(c) shows only nine curves for which the ratio of effective temperatures is smaller than 1. The ion distribution function is non-thermal, already quite different from a bi-Maxwellian with the same temperatures. Nevertheless, the results shown in Figure 1(c) are in some respects qualitatively similar to those appearing in Figure 1(a). However, despite these qualitative similarities, there are some significant differences. The values obtained for γ in the case of panel (c) show that the instability is very much increased by the non-thermal feature of the ion distribution function, as compared to the anisotropic Maxwellian case shown in Figure 1(a). The range of values of k which are unstable covers the region unstable in the Maxwellian case, but is extended toward the region $q \to 0$, for decreasing temperature ratio, and also seem to have a slightly extended upper limit. Moreover, it is noticed that the instability occurs even for temperature ratio 1.0, while for the Maxwellian case the instability started to appear only for temperature ratio smaller than 0.70, approximately. As example of the increase of the magnitude of the growth rates in the case of $\kappa_{i\perp} = \kappa_{i\|} = 5.0$, we may mention that for $T_{i/\perp}/T_{i\|} = 0.4$ (the magenta line in Figure 2(c)), which corresponds to effective temperature ratio 0.467, the maximum growth rate is about 0.05, a value which was obtained in the case of anisotropic Maxwellian distribution for the ions only for the much more anisotropic case of temperature ratio equal to 0.2, according to the results shown in Figure 1(a).

In Figures 1(d) and 1(h), we depict the results obtained considering the ions described by a strongly non-thermal product-bi-kappa distribution, with $\kappa_{\|} = \kappa_{\perp} = 2.5$ and $T_e = T_{i\|}$, and $T_{i\perp}/T_{i\|}$ ranging between 0.1 and 1.0, as in panels (a)–(c). The corresponding ratios of effective temperatures are $\theta_{i\perp}/\theta_{i\|} = 0.20$, 0.40, 0.60, 0.8, 1.0, 1.2, 1.4, 1.6, 1.8, and 2.0. The effective anisotropy is reversed for $T_{i\perp}/T_{i\|} \geq 0.5$, so that Figure 1(d) shows only four curves for which the ratio of effective temperatures is smaller than 1. The ion distribution function in this case is very different from a Maxwellian with the same temperature. The values obtained for γ in the case of Figure 1(d) show that the instability is very much increased by the non-thermal feature of the ion distribution function for most of the range of q values, when compared to the case of anisotropic Maxwellian shown in Figure 1(a). The range of values of k which are unstable is extended toward the region $q \to 0$, for the same temperature ratio, when compared to Figure 1(a), but the upper limit is decreased. The instability occurs for all values of the temperature ratio which has been considered, from 0.1 to 1.0, always with the same wave polarization, despite the fact that for temperature ratio above 0.5 the anisotropy is reversed in the ratio of effective temperatures. For the case of maximum temperature anisotropy which has been considered, $T_{i\perp}/T_{i\|} = 0.1$, which corresponds to ratio of effective temperatures equal to 0.2, the maximum growth rate is about 0.17, while for $T_{i\perp}/T_{i\|} = 0.2$ in the Maxwellian case, Figure 1(a), the maximum growth rate is much smaller, only about 0.08.

The values of the real part of the normalized wave frequency, z_r, corresponding to the values of z_i shown in

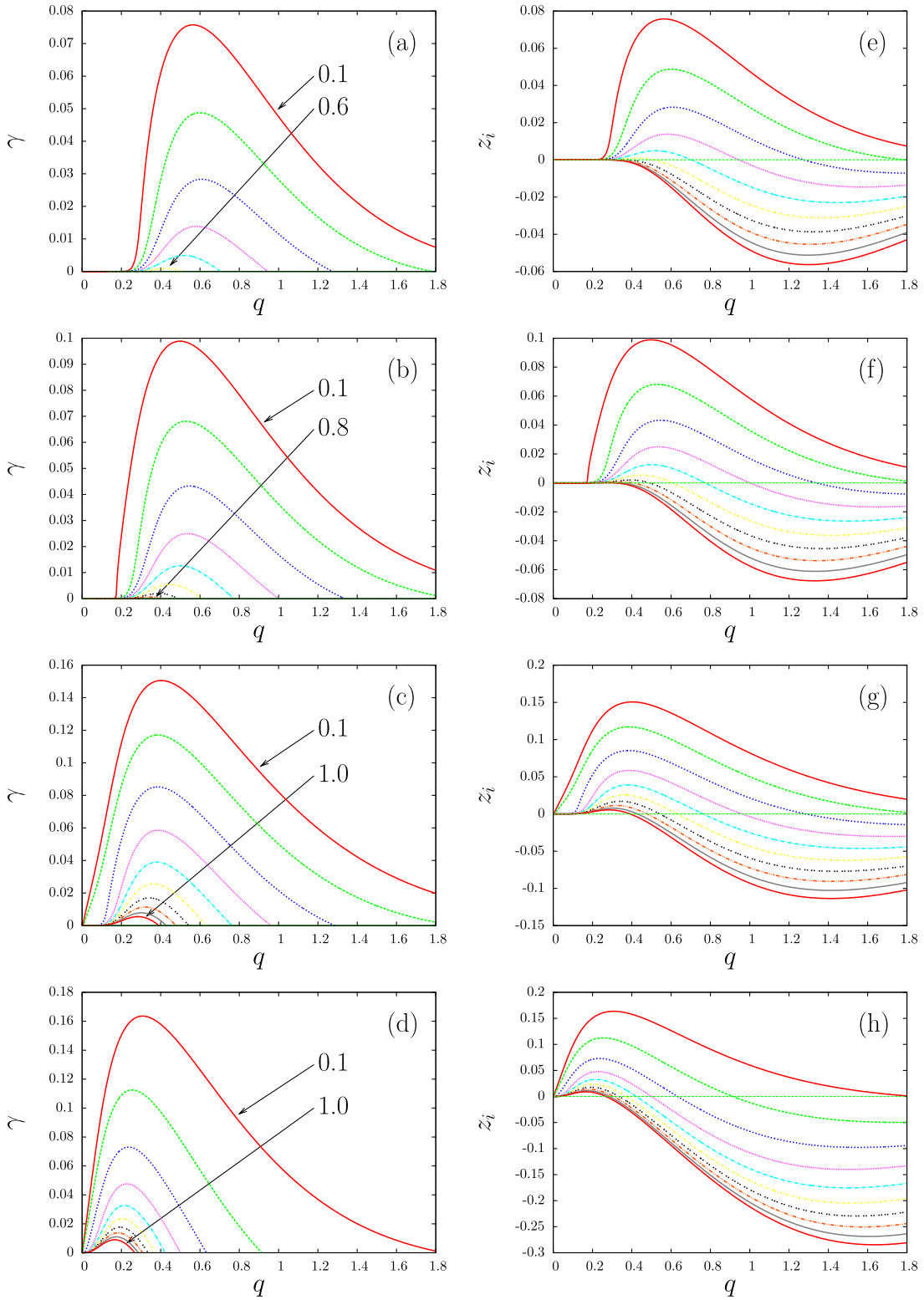

FIG. 1. Growth rate of instabilities (γ, left), and imaginary part of the normalized frequency (z_i, right), for waves in the whistler branch vs. normalized wave number, considering isotropic Maxwellian distributions for electrons and different forms of the ion distribution function. $\beta_i = 2.0$ and $v_A/c = 1.0 \times 10^{-4}$. (a) and (e) Anisotropic Maxwellian distribution for ions, for several values of the temperature ratio, $T_{i\perp}/T_{i\|} = 0.1$, 0.2, 0.3, 0.4, 0.5, 0.6, 0.7, 0.8, 0.9, and 1.0. (b) and (f) Ions with a product-bi-kappa distribution with $\kappa_{i\perp} = \kappa_{i\|} = 20$, for several values of the ratio $T_{i\perp}/T_{i\|} = 0.1$, 0.2, 0.3, 0.4, 0.5, 0.6, 0.7, 0.8, 0.9, and 1.0. (c) and (g) Ions with a product-bi-kappa distribution with $\kappa_{i\perp} = \kappa_{i\|} = 5.0$, for several values of the ratio $T_{i\perp}/T_{i\|} = 0.1$, 0.2, 0.3, 0.4, 0.5, 0.6, 0.7, 0.8, 0.9, and 1.0. (d) and (h) Ions with a product-bi-kappa distribution with $\kappa_{i\perp} = \kappa_{i\|} = 2.5$, for several values of the ratio $T_{i\perp}/T_{i\|} = 0.1$, 0.2, 0.3, 0.4, 0.5, 0.6, 0.7, 0.8, 0.9, and 1.0.

Figure 1, are depicted in Figure 2. The panels (a)–(d) of Figure 2 show the values of z_r corresponding to panels (a,e), (b,f), (c,g), and (d,h) of Figure 1.

Figure 3 analyses the effect of the form of the electron distribution function on the growth rate of the ion firehose instability, by showing the values of γ for waves in the

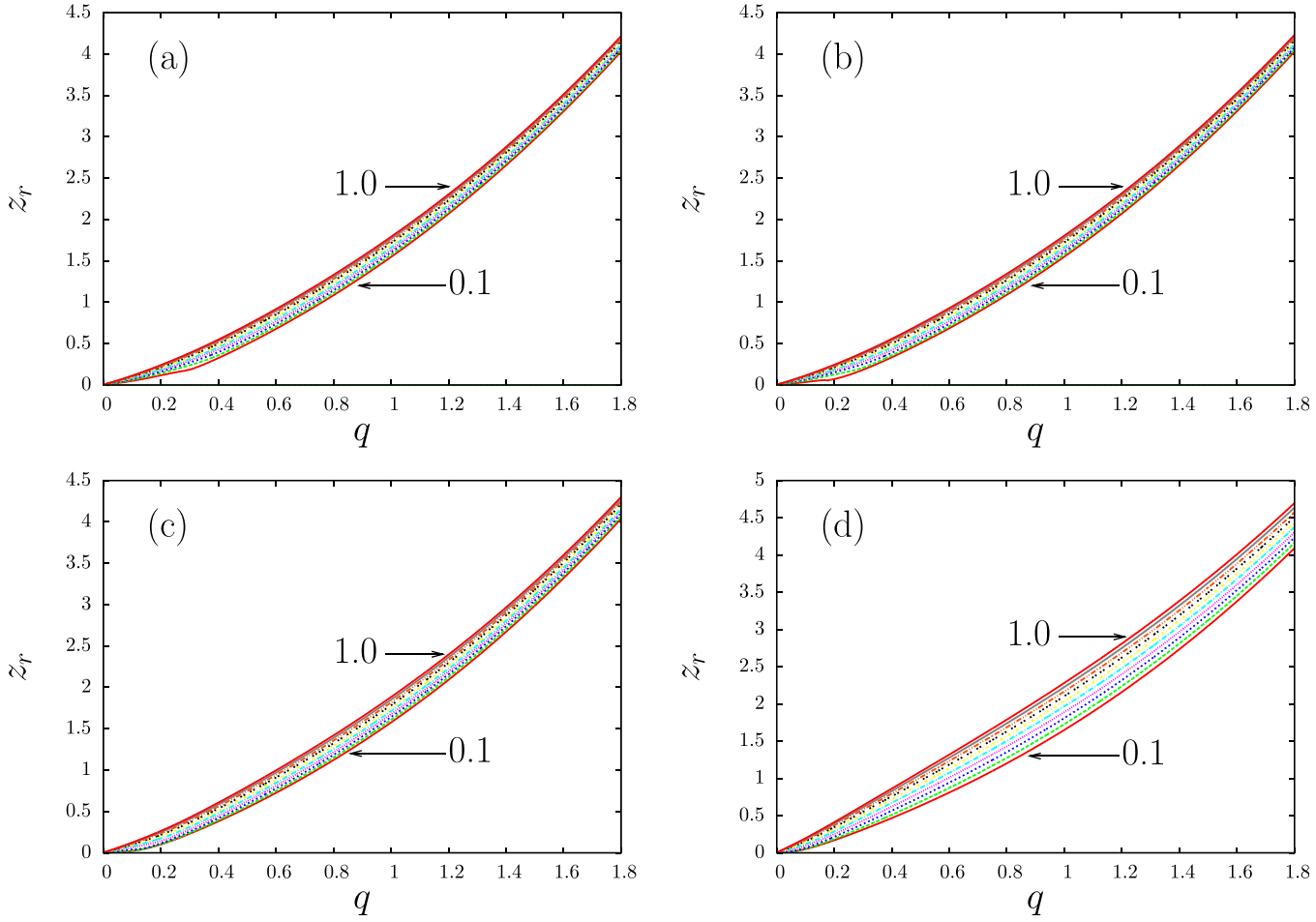

FIG. 2. Real part of the normalized frequency (z_r), for waves in the whistler branch vs. normalized wave number, considering isotropic Maxwellian distributions for electrons and different forms of the ion distribution function. The values of z_r which appear in this figure are the real counterparts to the values of z_i appearing in Figure 1. (a) Anisotropic Maxwellian distribution for ions, for several values of the temperature ratio, $T_{i\perp}/T_{i\|} = 0.1$, 0.2, 0.3, 0.4, 0.5, 0.6, 0.7, 0.8, 0.9, and 1.0. (b) Ions with a product-bi-kappa distribution with $\kappa_{i\perp} = \kappa_{i\|} = 20$, for several values of the ratio $T_{i\perp}/T_{i\|} = 0.1$, 0.2, 0.3, 0.4, 0.5, 0.6, 0.7, 0.8, 0.9, and 1.0. (c) Ions with a product-bi-kappa distribution with $\kappa_{i\perp} = \kappa_{i\|} = 5.0$, for several values of the ratio $T_{i\perp}/T_{i\|} = 0.1$, 0.2, 0.3, 0.4, 0.5, 0.6, 0.7, 0.8, 0.9, and 1.0. (d) Ions with a product-bi-kappa distribution with $\kappa_{i\perp} = \kappa_{i\|} = 2.5$, for several values of the ratio $T_{i\perp}/T_{i\|} = 0.1$, 0.2, 0.3, 0.4, 0.5, 0.6, 0.7, 0.8, 0.9, and 1.0.

whistler branch, obtained by considering a product-bi-kappa distribution for the ions and two different forms of the electron distribution function. In Figure 3(a), it is seen a case in which the electrons are characterized by an isotropic Maxwellian, and the ions are characterized by a product-bi-kappa distribution with $\kappa_{i\|} = \kappa_{i\perp} = 3.0$, with $T_{i\perp}/T_{i\|}$

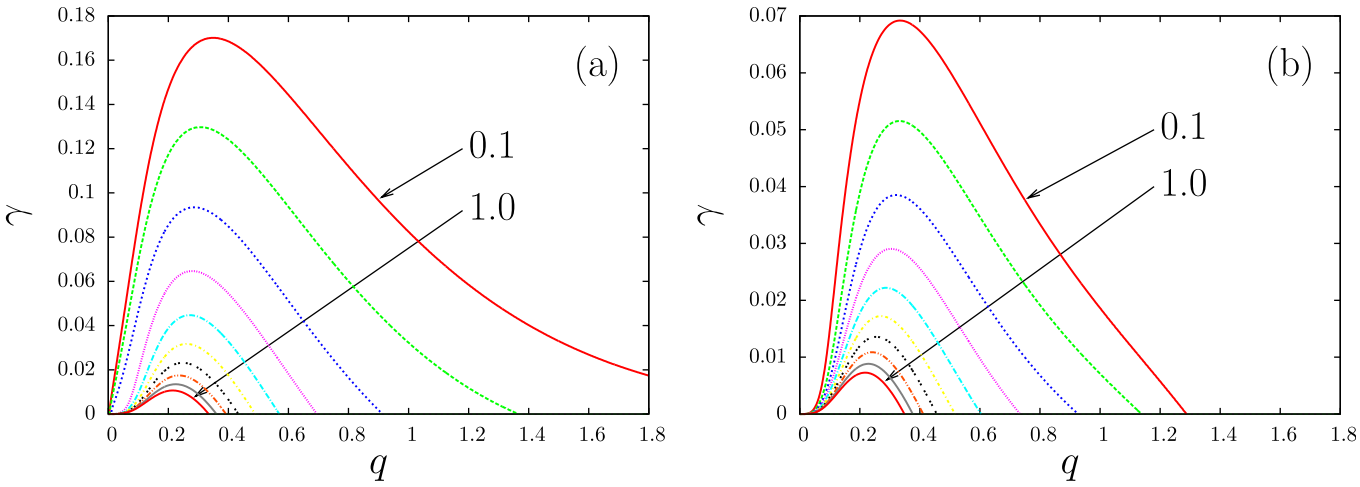

FIG. 3. Growth rate of instabilities (γ) for waves in the whistler branch, vs. normalized wave number. (a) Electrons with an isotropic Maxwellian distribution, ions with a product-bi-kappa distribution with $\kappa_{i\perp} = \kappa_{i\|} = 3.0$ and several values of the ratio $T_{i\perp}/T_{i\|} = 0.1$, 0.2, 0.3, 0.4, 0.5, 0.6, 0.7, 0.8, 0.9, and 1.0; (b) Electrons with a product-bi-kappa distribution with $\kappa_{e\perp} = \kappa_{e\|} = 3.0$ and $T_{e\perp} = T_{e\|}$; ions with a product-bi-kappa distribution with $\kappa_{i\perp} = \kappa_{i\|} = 3.0$ and several values of $T_{i\perp}/T_{i\|} = 0.1$, 0.2, 0.3, 0.4, 0.5, 0.6, 0.7, 0.8, 0.9, and 1.0.

ranging between 0.1 and 1.0. The situation is similar to that depicted in Figure 1(d), with the difference being the values of the κ indexes. The corresponding ratios of effective temperatures are $\theta_{i\perp}/\theta_{i\|} = 0.15$, 0.30, 0.45, 0.60, 0.75, 0.90, 1.05, 1.20, 1.35, and 1.50. In Figure 3(b), we consider a case in which the ion distribution is equal to that considered for Figure 3(a), but the electron distribution is also a product-bi-kappa distribution instead of a Maxwellian. We consider for Figure 3(b) the case of $\kappa_{e\|} = \kappa_{e\perp} = 3.0$, with isotropic temperatures, $T_{e\perp} = T_{e\|}$. The electron distribution is highly non-thermal, with extended "tails" along parallel and perpendicular directions. It is seen that the consequence of the modification in the electron distribution function is a meaningful decrease in the instability growth rate. For instance, the comparison between panels (b) and (a) of Figure 3 shows that, for $T_{i\perp} = T_{i\|} = 0.1$, the maximum growth rate has decreased from a value close to 0.18 to a value near 0.075, due to the change of the electron distribution function, from an isotropic Maxwellian, to a product-bi-kappa distribution with kappa indexes equal to 3.0, and isotropic temperatures. It is also noticed a sizable decrease of the unstable interval of wave numbers, specially for small values of the ratio $T_{i\perp}/T_{i\|}$. For instance, in the case of temperature ratio equal to 0.1, the upper limit of the unstable range is near $q = 1.2$ for the case of electrons described by a product-bi-kappa distribution with kappa index 3.0, and above $q = 1.8$ for the case of electrons described by a Maxwellian distribution. The inference is that, despite the fact that the instability is generated by the anisotropy in the ion distribution, the increase in the non-thermal feature of the electron distribution affects the instability, in this case reducing the growth rate.

Figure 4 is dedicated to discuss on the differences between the influences of the anisotropy due to the ratio of temperatures in the ion distribution and of the anisotropy due to the difference in the kappa indexes, also in the ion distribution. Figures 4(a) and 4(b) show the values of γ, obtained considering isotropic Maxwellian distribution for electrons and product-bi-kappa distributions for ions, with $\kappa_{i\perp} = \kappa_{i\|}$, for the values 3.0, 5.0, 10.0, 15.0, 20.0, and 25.0. Figure 4(a) shows the case of $T_{i\perp}/T_{i\|} = 0.435$, while Figure 3(b) shows the case of $T_{i\perp}/T_{i\|} = 0.50$. The comparison between these two cases of moderate anisotropy which are close to each other shows that, for a given value of the κ index, the unstable range of q tends to decrease with the decrease of the temperature anisotropy, and that the growth rates tend to decrease at each value of q. It is also seen that, for a given value of the temperature ratio, the maximum growth rate increases with the value of κ, from small κ until $\kappa \simeq 3$, and

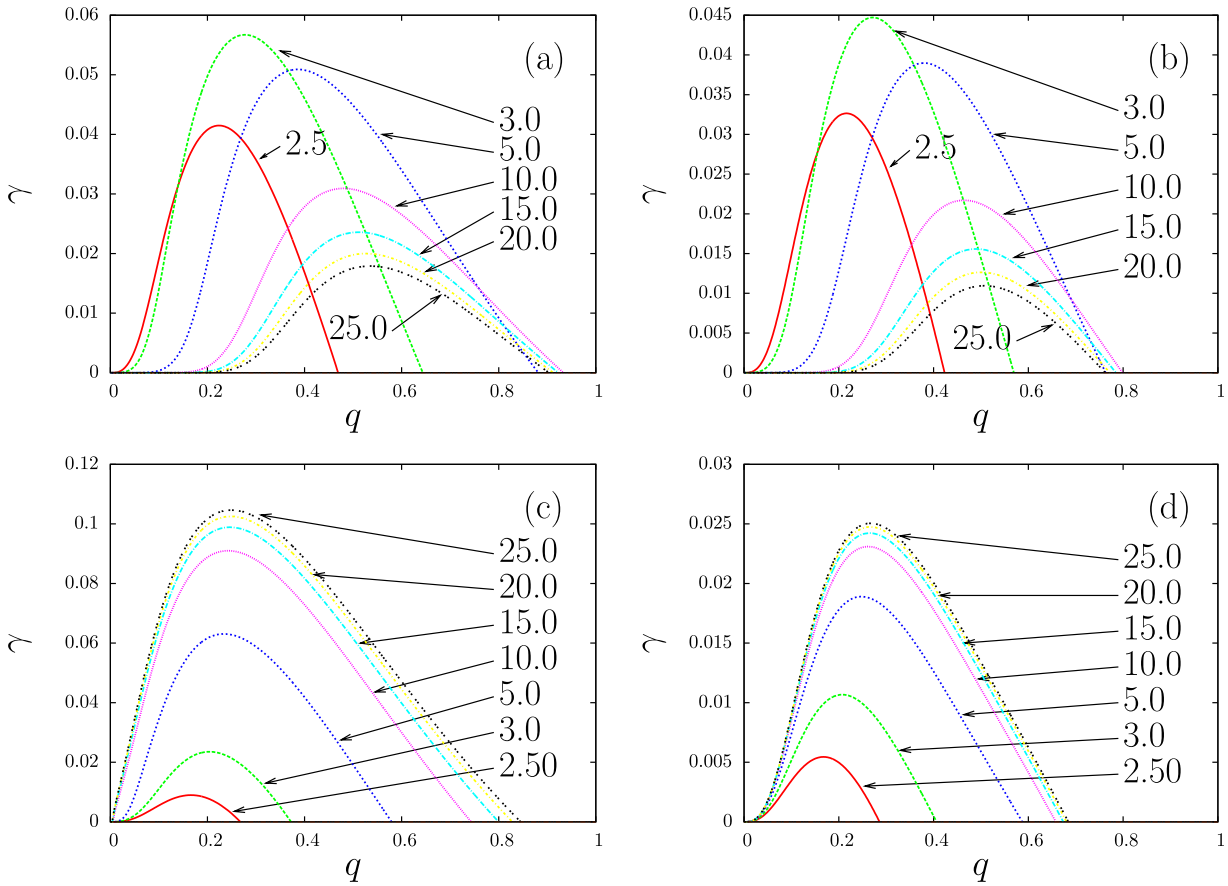

FIG. 4. Growth rate of instabilities (γ) for waves in the whistler branch, vs. normalized wave number. (a) Isotropic Maxwellian distribution for electrons and product-bi-kappa distribution for ions, with $T_{i\perp}/T_{i\|} = 0.435$ and several values of $\kappa_{i\perp} = \kappa_{i\|}$, 2.5, 3.0, 5.0, 10.0, 15.0, 20.0, and 25.0; (b) Isotropic Maxwellian distribution for electrons and product-bi-kappa distribution for ions, with $T_{i\perp}/T_{i\|} = 0.50$ and several values of $\kappa_{i\perp} = \kappa_{i\|}$, 2.5, 3.0, 5.0, 10.0, 15.0, 20.0, and 25.0; (c) Isotropic Maxwellian distribution for electrons and product-bi-kappa distribution for ions, with $T_{i\perp}/T_{i\|} = 1.0$, $\kappa_{i\|} = 2.5$, and several values of $\kappa_{i\perp}$, 2.5, 3.0, 5.0, 10.0, 15.0, 20.0, and 25.0 (values of $\theta_{i\perp}/\theta_{i\|}$ are 2.0, 1.2, 0.67, 0.50, 0.46, 0.444, and 0.435); (d) Product-bi-kappa distribution for electrons, with $T_{e\perp}/T_{e\|} = 1.0$ and $\kappa_{e\|} = \kappa_{e\perp} = 2.5$, and product-bi-kappa distribution for ions, with $T_{i\perp}/T_{i\|} = 1.0$, $\kappa_{i\|} = 2.5$, and several values of $\kappa_{i\perp}$, 2.5, 3.0, 5.0, 10.0, 15.0, 20.0, and 25.0.

then decreases and tends to a limiting value for very large value of κ, which is smaller than the maximum γ for $\kappa = 3$.

In Figure 4(c), we explore the anisotropy due to different values of $\kappa_{i\perp}$ and $\kappa_{i\parallel}$, by considering a case in which $T_{i\perp}/T_{i\parallel} = 1.0$, with $\kappa_{i\parallel} = 2.5$ and $\kappa_{i\perp} = 2.5$, 3.0, 5.0, 10.0, 15.0, 20.0, and 25.0, with isotropic Maxwellian for the electrons. The increase in $\kappa_{i\perp}$, for small $\kappa_{i\parallel}$, corresponds to a decrease in perpendicular effective temperature, and therefore to an increase of the anisotropy in the distribution function (the corresponding values of $\theta_{i\perp}/\theta_{i\parallel}$ are 2.0, 1.2, 0.67, 0.50, 0.46, 0.444, and 0.435). It is seen the tendency of the ratio of effective temperatures to saturate at 0.4, for $\kappa_{i\perp} \to \infty$. In terms of the effective anisotropy, the dashed blue curve in Figure 4(c), obtained with $\kappa_{i\parallel} = 2.5$ and $\kappa_{i\perp} = 25.0$ ($\theta_{i\perp}/\theta_{i\parallel} = 0.435$), should be compared to the full line red curve in Figure 4(a), also obtained with $\kappa_{i\parallel} = 2.5$, but with anisotropy due to $T_{i\perp}/T_{i\parallel} = 0.435$. It is seen that in panel (c) the instability for this case occurs from $q = 0$ to $q \simeq 0.8$, with maximum growth rate $\gamma \simeq 0.11$, while in panel (a) the instability for the comparing case is restricted to the region $q \leq 0.45$, with maximum value $\gamma \simeq 0.045$. The instability is very much increased in range and magnitude, for anisotropy due to the anisotropic κ parameters, as compared to the case of anisotropy due to anisotropic temperature parameters. This conclusion can also be drawn from other curves. For instance, the fourth curve in Figure 4(c), the magenta line, corresponds to $\theta_{i\perp}/\theta_{i\parallel} = 0.50$, and should be compared with the full red line in Figure 4(b), obtained for $T_{i\perp}/T_{i\parallel} = 0.50$. It is seen that the instability in the case of panel (c) extends over a larger interval of q values, with considerably larger growth rate.

In Figure 4(d), we consider a situation where the ion distribution function is the same as in Figure 4(c), but the electron distribution is a product-bi-kappa distribution, with $T_{e\perp} = T_{e\parallel}$ and $\kappa_{e\perp} = \kappa_{e\parallel} = 2.5$. The comparison between Figures 4(c) and 4(d) show that the appearing of non-thermal kappa-like features in the electron distribution contributes to decrease the instability, which is caused by the anisotropy in the ion distribution. The situation regarding the effect of the shape of the electron distribution, in the case of Figure 4, where the anisotropy is due to anisotropic κ indexes in the ion distribution, is similar to the situation depicted in Figure 3(a), in which the anisotropy was due to the difference between $T_{i\perp}$ and $T_{i\parallel}$.

In Figure 5, we analyse the effect of the parameter β_i, by considering situations which are similar to those considered

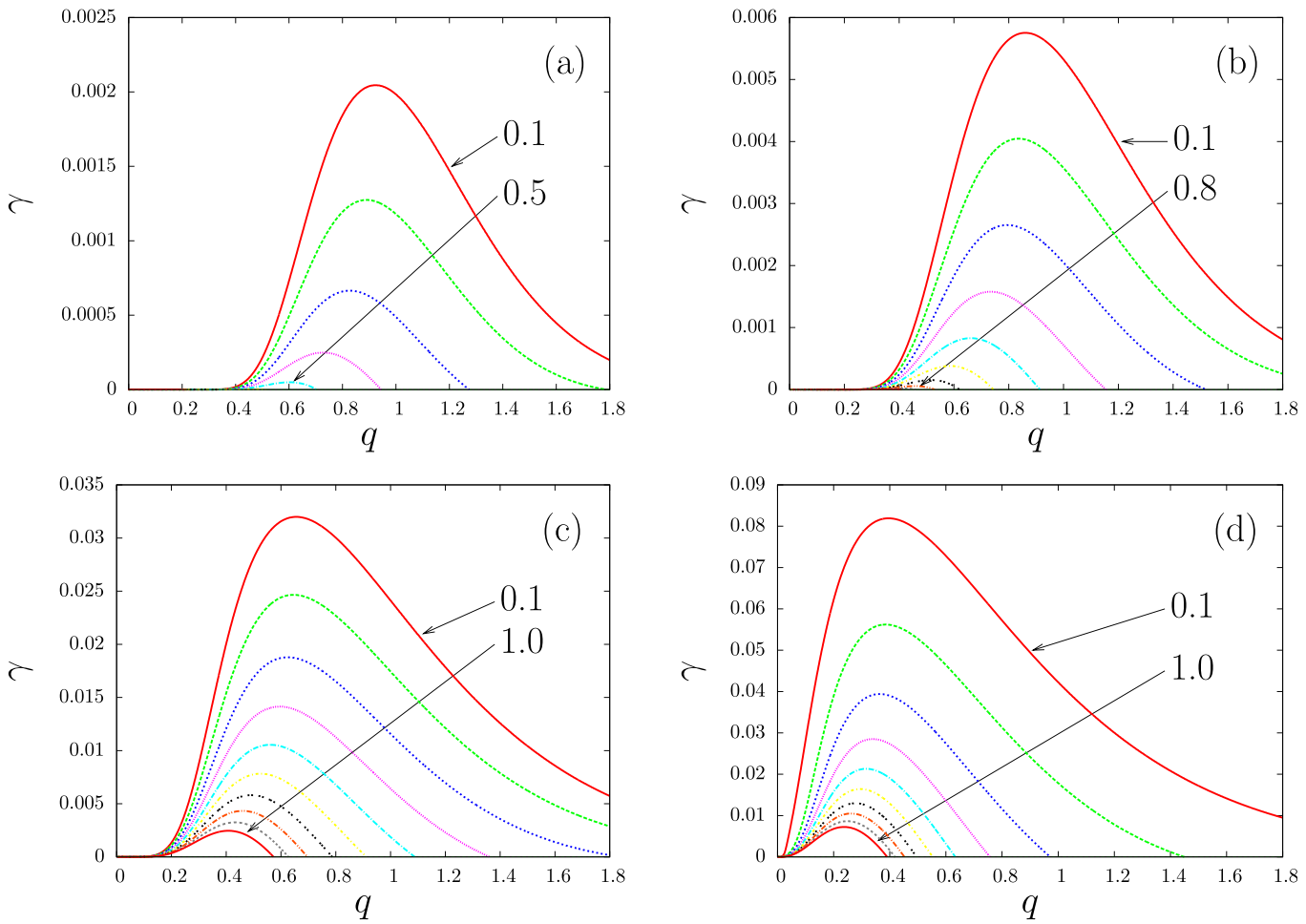

FIG. 5. Growth rate of instabilities (γ) for waves in the whistler branch vs. normalized wave number, considering isotropic Maxwellian distributions for electrons and different forms of the ion distribution function. $\beta_i = 1.0$ and $v_A/c = 1.0 \times 10^{-4}$. (a) Anisotropic Maxwellian distribution for ions, for several values of the temperature ratio, $T_{i\perp}/T_{i\parallel} = 0.1$, 0.2, 0.3, 0.4, 0.5, 0.6, 0.7, 0.8, 0.9, and 1.0; (b) Ions with a product-bi-kappa distribution with $\kappa_{i\perp} = \kappa_{i\parallel} = 20$, for several values of the ratio $T_{i\perp}/T_{i\parallel} = 0.1$, 0.2, 0.3, 0.4, 0.5, 0.6, 0.7, 0.8, 0.9, and 1.0; (c) Ions with a product-bi-kappa distribution with $\kappa_{i\perp} = \kappa_{i\parallel} = 5.0$, for several values of the ratio $T_{i\perp}/T_{i\parallel} = 0.1$, 0.2, 0.3, 0.4, 0.5, 0.6, 0.7, 0.8, 0.9, and 1.0; (d) Ions with a product-bi-kappa distribution with $\kappa_{i\perp} = \kappa_{i\parallel} = 2.5$, for several values of the ratio $T_{i\perp}/T_{i\parallel} = 0.1$, 0.2, 0.3, 0.4, 0.5, 0.6, 0.7, 0.8, 0.9, and 1.0.

for Figure 1, with the difference that we now use $\beta_i = 1.0$ instead of $\beta_i = 2.0$. The sequence of panels appearing in Figure 5 shows results which can be qualitatively described as those of the left panels of Figure 1. However, the decrease of the factor β_i has caused a strong decrease in the magnitude of the growth rates. For instance, for the case shown in panel (a) with $T_{i\perp}/T_{i\|} = 0.1$, the case of $\beta_i = 2.0$ features maximum value $\gamma \simeq 0.076$, while the case of $\beta_i = 1.0$ leads to maximum value of $\gamma \simeq 0.002$. Moreover, it is noticed that for the smaller value of β_i the magnitude of the effect associated to the non-thermal character of the distribution in clearly enhanced. For instance, the peak value of γ appearing in Figure 5(b) is about 0.0058, while in Figure 5(a) it is nearly 0.002, smaller by almost a factor of three. For the case of $\beta_i = 2$, Figures 1(b) and 1(a) show that the corresponding values are 0.099 and 0.077, a difference less than 30%. Another example can be obtained from the comparison between panels (d) and (c) in Figure 5. It is seen that the value at the peak of γ in panel (d) is more than twice the value at the peak in panel (c). It is also seen that the points of maximum growth are displaced toward smaller q, with the instability reaching $q = 0$ in panel 5(d). In the case of Figure 1, the maximum values of γ in (d) and (c) differ by less than 10%, and the displacement of the instability toward smaller values of q is less significant than in the case of Figure 5.

Finally, we compare the results obtained from the dispersion relation considering product-bi-kappa distributions with results obtained from the dispersion relation considering bi-kappa distributions, defined as follows:

$$f^{(0)}_{\beta,\kappa}(v_\|, v_\perp) = \frac{1}{\pi^{3/2}\kappa_\beta^{3/2} v^2_{\beta\perp} v_{\beta\|}} \frac{\Gamma(\kappa_\beta)}{\Gamma(\kappa_\beta - 3/2)} \times \left(1 + \frac{v_\|^2}{\kappa_\beta v^2_{\beta\|}} + \frac{v_\perp^2}{\kappa_\beta v^2_{\beta\perp}}\right)^{-\kappa_\beta}, \quad \left(\kappa_\beta > \frac{3}{2}\right). \tag{17}$$

If all plasma species are described by distribution functions as defined by Eq. (17), the dispersion relation for parallel propagating low frequency electromagnetic waves becomes as follows:

$$N_\|^2 = 1 + \frac{1}{z^2}\sum_\beta \frac{\omega^2_{p\beta}}{\Omega_i^2}\left[-1 + \frac{u^2_{\beta\perp}}{u^2_{\beta\|}} + \left(\zeta^0_\beta - \zeta^s_\beta + \frac{u^2_{\beta\perp}}{u^2_{\beta\|}}\zeta^s_\beta\right)\frac{\kappa_\beta - 3/2}{\kappa_\beta - 1} Z^{(-1)}_\kappa(\zeta^s_\beta)\right]. \tag{18}$$

If different species are described by different forms or the distribution function, either Maxwellian, bi-kappa (Eq. (17)), of product-bi-kappa (Eq. (4)), the dispersion relation has to be written using a proper combination of terms.

In Figure 6, we show a comparison between the growth rates associated with product-bi-kappa distributions and those associated to bi-kappa distributions. In Figure 6(a), we consider an isotropical Maxwellian distribution for electrons, and two different forms of the ion distribution function. The curves with dashed lines in Figure 6(a) are obtained considering a PBK distribution with $\kappa_{i\perp} = \kappa_{i\|} = 20$ to describe the ions, for several values of the ion temperature ratio, $T_{i\perp}/T_{i\|} = 0.1$, 0.2, 0.3, 0.4, 0.5, and 0.6. These dashed curves correspond to those of Figure 1(b). The continuous lines in Figure 6(a) are obtained considering a BK distribution with $\kappa_i = 20$ to describe the ions, for the same values of the temperature ratios used for the dashed lines. The results shown in Figure 6(a) show that for large anisotropy (temperature ratio ≤ 0.4) the peak value of the growth rate is larger in the case of BK distributions than for PBK distributions. For temperature ratios 0.5 and 0.6, however, the results show that the situation is reversed. The maximum growth rate is larger in the case of PBK distribution than in the case of BK distribution. It is also seen that for these values of the temperature ratio above 0.4 the upper limit of the region of unstable wave number is smaller in the case of BK distribution than in the case of PBK distribution, with the difference increasing with the temperature ratio.

In Figure 6(b) we compare results obtained considering ions with PBK distributions with $\kappa_{i\perp} = \kappa_{i\|} = 5$ with results obtained considering ions with BK distributions with $\kappa_i = 5$, with isotropic Maxwellian distribution for the electrons, for ion temperature ratios 0.1, 0.2, 0.3, 0.4, 0.5, 0.6, 0.7, 0.8, and 0.9. The dashed curves in Figure 6(b) correspond to those in Figure 1(c). The comparison between the results shown in Figures 6(b) and 6(a) shows that the magnitude of the growth rates increase with the decrease of the kappa values, both for PBK and for BK distributions. It is also seen that the magnitude of the difference between the results obtained with the two forms of the ion distribution function increases with the decrease of the kappa indexes. For temperature ratio 0.1 the maximum growth rate obtained with PBK distribution is nearly 25% smaller than obtained with BK distribution. For temperature ratio 0.5 the maximum growth rate is about 0.7 for BK distribution and 0.4 for PBK distribution, about 60% of the value obtained with the PBK. The situation is reversed with the increase of the temperature ratio, so that for 0.7 the maximum growth rate is larger for PBK than for BK, with much larger range of unstable wavenumbers. For small anisotropy, like in the case of temperature ratio 0.9, the instability disappears in the case of BK distribution, but remains in the case of PBK distribution, for normalized wavenumber between 0.1 and 0.42.

In Figures 6(c) and 6(d), we further investigate the effect of the shape of the electron distribution. In the case of Figure 6(c), the ion distributions are the same as in Figure 6(a), but the electron distribution is a BK with $\kappa_e = 20$ in the case of the continuous lines, and a PBK with $\kappa_{e\perp} = \kappa_{e\|} = 20$ in the case of the dashed lines. The comparison between the continuous lines in Figures 6(a) and 6(c) show that in the case of BK ion distributions the growth rates are not affected by the change of the electron distribution, from a Maxwellian to a BK distribution. The dashed lines, on the other hand, show some reduction of the growth rate obtained with ion PBK distribution, due to the change in the electron distribution function. For instance, the dashed lines show that the maximum value of γ in the case of $T_{i\perp}/T_{i\|} = 0.1$ is about 0.1 in panel (a), with Maxwellian electrons, and about 0.09 in panel (c), with PBK electrons.

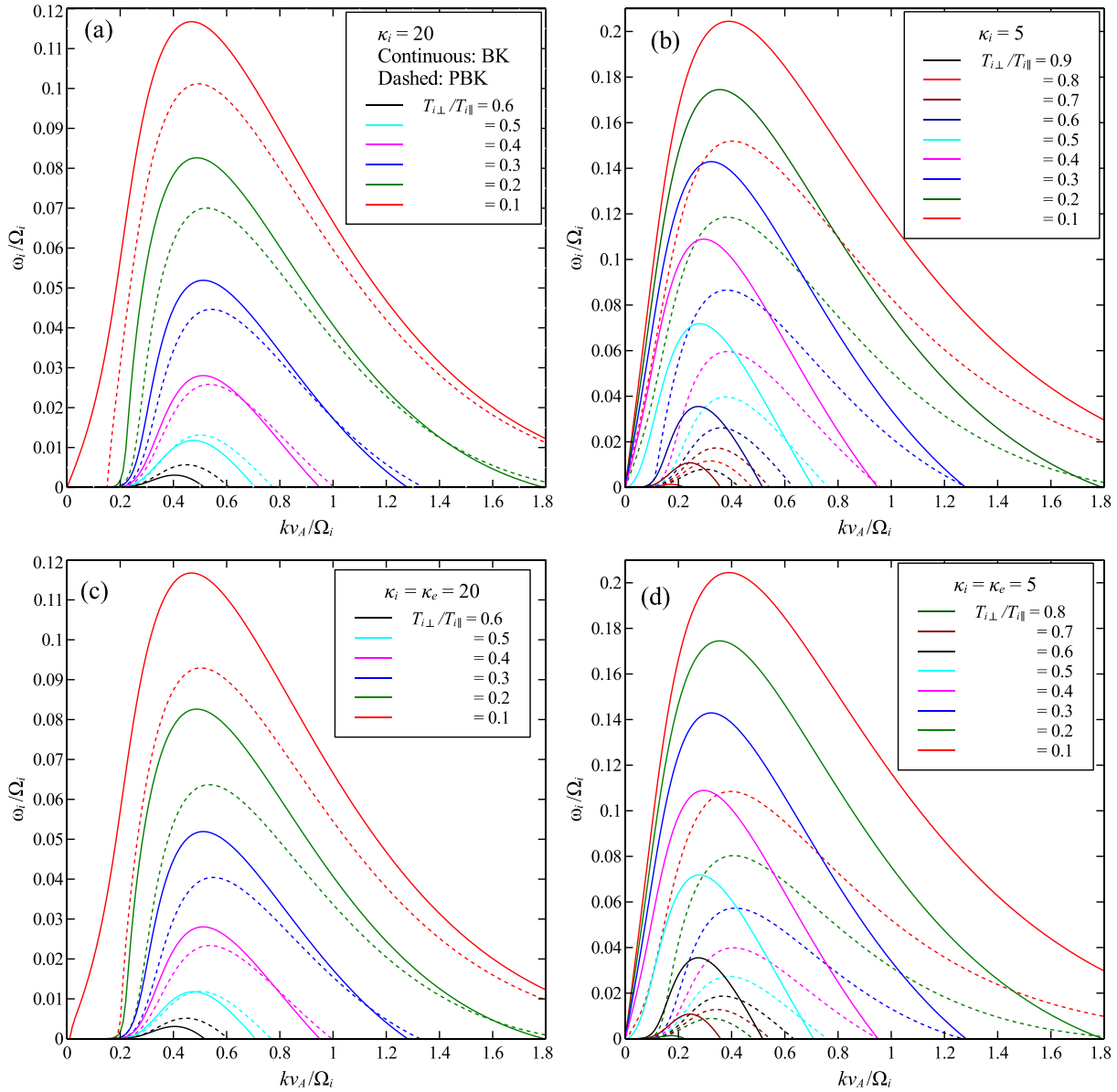

FIG. 6. Growth rate of instabilities (γ) for waves in the whistler branch vs. normalized wave number, obtained by considering two different forms of the ion distribution function, for $\beta_i = 2.0$ and $v_A/c = 1.0 \times 10^{-4}$. (a) Dashed lines: Obtained with ions with a product-bi-kappa distribution with $\kappa_{i\perp} = \kappa_{i\|} = 20$, and isotropical Maxwellian distribution for electrons; continuous lines: Obtained with ions with a bi-kappa distribution with $\kappa_i = 20$, and isotropical Maxwellian distribution for electrons. In both cases, the temperature ratios are $T_{i\perp}/T_{i\|} = 0.1$, 0.2, 0.3, 0.4, 0.5, and 0.6. (b) Dashed lines: Obtained with ions with a product-bi-kappa distribution with $\kappa_{i\perp} = \kappa_{i\|} = 5$, and isotropical Maxwellian distribution for electrons; continuous lines: Obtained with ions with a bi-kappa distribution with $\kappa_i = 5$, and isotropical Maxwellian distribution for electrons. In both cases, the temperature ratios are $T_{i\perp}/T_{i\|} = 0.1$, 0.2, 0.3, 0.4, 0.5, 0.6, 0.7, 0.8, and 0.9. (c) Dashed lines: Obtained with ions with a product-bi-kappa distribution with $\kappa_{i\perp} = \kappa_{i\|} = 20$, and electrons with product-bi-kappa distribution with $\kappa_{e\perp} = \kappa_{e\|} = 20$; continuous lines: Obtained with ions with a bi-kappa distribution with $\kappa_{i\perp} = \kappa_{i\|} = 20$, and electrons with product-bi-kappa distribution with $\kappa_{e\perp} = \kappa_{e\|} = 20$; In both cases, the temperature ratios are $T_{i\perp}/T_{i\|} = 0.1$, 0.2, 0.3, 0.4, 0.5, and 0.6. (d) Dashed lines: Obtained with ions with a product-bi-kappa distribution with $\kappa_{i\perp} = \kappa_{i\|} = 5$, and electrons with product-bi-kappa distribution with $\kappa_{e\perp} = \kappa_{e\|} = 5$; continuous lines: Obtained with ions with a bi-kappa distribution with $\kappa_{i\perp} = \kappa_{i\|} = 5$, and electrons with product-bi-kappa distribution with $\kappa_{e\perp} = \kappa_{e\|} = 5$; In both cases, the temperature ratios are $T_{i\perp}/T_{i\|} = 0.1$, 0.2, 0.3, 0.4, 0.5, 0.6, 0.7, and 0.8.

In Figure 6(d), we consider a case in which the ion distributions are as in Figure 6(b), but the electron distribution is a BK with $\kappa_e = 5$ (continuous lines) or a PBK with $\kappa_{e\perp} = \kappa_{e\|} = 5$ (dashed lines). As in the case od $\kappa = 20$ shown in Figure 6(c), the comparison of the continuous line in Figure 6(d) with those of Figure 6(b) show that the increase of the non-thermal character of the electron distribution, associated to the BK distribution, does not affect the growth rate of the instability. On the other hand, the dashed curves in these figures show that in the case of ions with a PBK distribution the modification of the electron distribution, from a Maxwellian distribution to a PBK distribution, makes the growth rate of the ion firehose instability to be reduced in a significant way. For instance, the maximum value of γ in the case of temperature ratio 0.1 is about 0.15 if the electron distribution is Maxwellian, panel (b), and about 0.1 if the electron distribution is a PBK with $\kappa_{e\perp} = \kappa_{e\|} = 5.0$.

The results obtained also have indicated that the instability is very much increased, in wave number range and in magnitude, if the anisotropy in the distribution is caused by

anisotropy in the κ indexes, instead of by anisotropy in parallel and perpendicular temperatures.

IV. FINAL REMARKS

In the present paper, we have presented some results originated from numerical analysis of the dispersion relation for low frequency electromagnetic waves propagating parallel to the ambient magnetic field, considering that the velocity distributions of ions and electrons can be either bi-Maxwellian of product bi-kappa distributions. The analysis is centered on the behavior of waves in the whistler mode and on the so-called ion firehose instability.

The results obtained show that the ion firehose instability is very much increased when the non-thermal feature of the product-bi-kappa distribution is associated to the plasma ions, as compared to the results obtained when the ion distribution is an anisotropic Maxwellian distribution. The range of values of wave number which are unstable covers the region unstable in the bi-Maxwellian case, but increases toward the region of large wavelengths for decreasing κ indexes, for sufficiently low values of the temperature ratio $T_{i\perp}/T_{i\|} < 1$. According to the numerical analysis which has been made, these effects associated to the non-thermal character of the product-bi-kappa ion distribution are clearly enhanced with the decrease of the plasma parameter β_i.

Our results have also shown that in the case of product-bi-kappa ion distribution the instability occurs even for temperature ratio 1.0 and equal κ indexes, $\kappa_{i\perp} = \kappa_{i\|}$, due to the anisotropy which is inherent to the product-bi-kappa distribution. As it is known, for the bi-Maxwellian case the occurrence of the instability requires some degree of anisotropy in the temperature.

We have also investigated the effect of the electron distribution function on the growth rate of the instability. Our results have shown that, despite the fact that the ion firehose instability is driven by anisotropy in the ion distribution, the increase in the non-thermal feature of the electron distribution which is associated to product-bi-kappa distribution affects the instability, with significant reduction of the growth rate.

We have also analyzed the effect of different forms of the non-thermal distribution by comparing results obtained considering product-bi-kappa distributions with results obtained considering bi-kappa distributions, with similar values of the κ indexes. The growth rates obtained from the dispersion relations show complex behaviour, regarding the shape of the ion distribution, even if the electron distribution is considered an isotropical Maxwellian. For small values of the temperature ratio the growth rate is larger for BK than for PBK distributions, but the situation is reversed when the ion temperature ratio approaches unity. Very significant effects have also been obtained when the electron distribution has also been considered with non-thermal character. It has been seen that the adoption of a BK distribution with isotropic temperature for the electrons, instead of a Maxwellian, does not affect the growth rates of the instability, while the adoption of electrons with a PBK distribution, even with isotropic temperature, contributes do decrease the intensity of the instability. The magnitude of the effect is increased with the reduction of the κ indexes, so that the instability is very much quenched in the case of electron distributions with small κ indexes.

These findings relative to the sensitivity of the growth rates of the ion firehose instability on the detailed form of a power-law electron distribution can be of consequence on analysis of the instability threshold in the space plasma environment. Although it is already recognized that anisotropies in the electron distribution can affect the threshold for instabilities which are driven by anisotropies in the ion distribution,[20,23] the analysis of observed data has been generally made by considering bi-Maxwellian of bi-kappa distributions, which miss anisotropy features that can be associated to PBK distributions. As we have seen, these features lead to relevant effects on the evaluation of the growth rate of the ion firehose instability.

The results which are shown in the present paper demonstrate that apparently small differences in the distribution functions of plasma particles can lead to significant differences in the magnitude of the growth rates and in the range of wave numbers which feature the so-called ion firehose instability. The inference is that product-bi-kappa distributions, with inherent flexibility for modeling due to the possibility of different values of the parallel and perpendicular κ indexes and of the values of the parallel and perpendicular temperatures, can be useful for analysis of wave phenomena in the space environment, frequently made considering combinations of Maxwellian distributions.

Analyses similar to those presented here are being performed in order to describe the effect of product-bi-kappa distribution on other instabilities occurring for low-frequency electromagnetic waves, as the ion-cyclotron instability and the electron firehose instability. Corresponding studies considering the presence of dust are also being performed and shall be reported in a forthcoming publication.

ACKNOWLEDGMENTS

This work has received partial support from Brazilian agencies CNPq and CAPES.

[1]S. P. Gary, *Theory of Space Plasma Microinstabilities*, Cambridge Atmospheric and Space Science Series (Cambridge University Press, New York, 2005).
[2]S. P. Gary, H. Li, S. O'Rourke, and D. Winske, J. Geophys. Res. **103**, 14567, doi:10.1029/98JA01174 (1998).
[3]M. C. de Juli, R. S. Schneider, L. F. Ziebell, and R. Gaelzer, J. Geophys. Res. **112**, A10105, doi:10.1029/2007JA012434 (2007).
[4]J. C. Kasper, A. J. Lazarus, and S. P. Gary, Geophys. Res. Lett. **29**, 1839, doi:10.1029/2002GL015128 (2002).
[5]J. C. Kasper, A. J. Lazarus, S. P. Gary, and A. Szabo, in *Proceedings of the Tenth International Solar Wind Conference* (2003), Vol. 679, p. 538.
[6]W. Pilipp, H. Miggenrieder, M. Montgomery, K.-H. Mühlhäuser, H. Rosenbauer, and R. Schwenn, J. Geophys. Res. **92**, 1075, doi:10.1029/JA092iA02p01075 (1987).
[7]W. Pilipp, H. Miggenrieder, M. Montgomery, K.-H. Mühlhäuser, H. Rosenbauer, and R. Schwenn, J. Geophys. Res. **92**, 1093, doi:10.1029/JA092iA02p01093 (1987).
[8]E. Marsch, X.-Z. Ao, and C.-Y. Tu, J. Geophys. Res. Space Phys. **109**, A04102 (2004).
[9]E. Marsch, Living Rev. Sol. Phys. **3**, 1 (2006).
[10]V. M. Vasyliunas, J. Geophys. Res. **73**, 2839, doi:10.1029/JA073i009p02839 (1968).
[11]D. Summers and R. M. Thorne, Phys. Fluids B **3**, 1835 (1991).

[12]R. L. Mace and M. A. Hellberg, Phys. Plasmas **2**, 2098 (1995).
[13]M. P. Leubner, Astrophys. Space Sci. **282**, 573 (2002).
[14]M. P. Leubner, Astrophys. J. **604**, 469 (2004).
[15]V. Pierrard and M. Lazar, Sol. Phys. **267**, 153 (2010).
[16]M. Lazar, Astron. Astrophys. **547**, A94 (2012).
[17]M. Lazar and S. Poedts, Mon. Not. R. Astron. Soc. **437**, 641 (2014).
[18]M. Lazar and S. Poedts, Astron. Astrophys. **494**, 311 (2009).
[19]M. Lazar and S. Poedts, Sol. Phys. **258**, 119 (2009).
[20]M. Lazar, S. Poedts, and R. Schlickeiser, Astron. Astrophys. **534**, A116 (2011).
[21]M. Lazar, V. Pierrard, S. Poedts, and R. Schlickeiser, Astrophys. Space Sci. Proc. **33**, 97 (2012).
[22]R. A. Galvão, L. F. Ziebell, R. Gaelzer, and M. C. de Juli, Braz. J. Phys. **41**, 258 (2011).
[23]M. J. Michno, M. Lazar, P. H. Yoon, and R. Schlickeiser, Astrophys. J. **781**, 49 (2014).